EVALUATION OF A MODIFIED MICA AND MONTMORILLONITE FOR THE ADSORPTION OF IBUPROFEN FROM AQUEOUS MEDIA

Julia Martín[1], María del Mar Orta[2*], Santiago Medina-Carrasco[3], Juan Luis Santos[1], Irene Aparicio[1], Esteban Alonso[1]

[1]*Department of Analytical Chemistry, Escuela Politécnica Superior, University of Seville. E–41011 Seville, Spain.*

[2]*Department of Analytical Chemistry, Faculty of Pharmacy, University of Seville, E-41012 Seville, Spain.*

[3]*X-Ray Laboratory (CITIUS), University of Seville, E-41012 Seville, Spain.*

*Corresponding author: María del Mar Orta

Address:

Department of Analytical Chemistry, Faculty of Pharmacy, University of Seville, E-41012 Seville, Spain.

E-mail: enmaorta@us.es

Phone-number: +34-9-5455-3804

Abstract

The goals of this work were to prepare and characterize two functional materials, a natural montmorillonite (Mt) and a synthetic mica (Na-mica-4) were modified with the cationic octadecylamine by a cation-exchange reaction between obtained C_{18}-Mt and C_{18}-mica-4, and to explore their potential uses as adsorbent of water containing emerging compounds such as ibuprofen.

Both materials were characterized by X-ray diffraction (XRD), Zeta potential and thermogravimetric analysis (DSC-TG), before and after adsorption experiments. The incorporation of ibuprofen in the interlayer was demonstrated by XRD and on the external surface by Zeta potential.

The adsorption equilibrium isotherm was fitted with the Langmuir, Freundlich and Dubinin-Radushkevitch mathematical models to obtain the respective parameters. Langmuir and Freundlich were the models that best fitted the experimental data (R^2> 0.999). The adsorption rate of C_{18}-Mt (99.9%) was not dependent of ibuprofen concentration (0.1-80 mg/L) but it was in the case of C_{18}-mica-4 (from 99.9% at 0.1 mg/L to 67% at 80 mg/L). In addition, these values were not affected by sample pH in the range from 4 to 9. Kinetic of ibuprofen adsorption onto the organoclays was evaluated using pseudo-first-order, pseudo-second-order, intra-particle diffusion and Elovich models. Pseudo-second order was the kinetic model that best described the adsorption of ibuprofen (R^2> 0.993) reaching the equilibrium time (up to 100% adsorbed) in less than 5 min and 60 min for C_{18}-Mt and C_{18}-mica-4, respectively. The mechanistic study confirmed the validity of these materials for the uptake of ibuprofen from water.

Keywords: *Ibuprofen; Adsorption; C_{18}-Montmorillonite; C_{18}-mica-4; Water samples*

1. Introduction

Pharmaceutical wastewaters are very hazardous and toxic not only for the human but also for environmental life (Wilkinson et al., 2017; Tarpani and Azapagic, 2018; Tran et al., 2018). They are still not included in routine monitoring programs, but were added to the Candidates Contaminant List for prioritizing their regulation in near future (Directive 2013/39/EU; Sousa et al., 2018). Ibuprofen is among the most frequently reported active pharmaceutical ingredients in ambient monitoring studies and consistently detected in finished drinking water at high concentrations (>1 μg/L) (Vieno et al., 2005; Loraine and Pettigrove, 2006; Mompelat et al., 2009). This is due to its high consumption allied with the poor efficiency of conventional water treatment processes for its complete removal/degradation (Mompelat et al., 2009; Martín et al., 2011; Carvalho et al., 2013; Yang et al., 2017; Tarpani and Azapagic, 2018). Several methods have been investigated to remove pharmaceuticals from contaminated water such as ultrasonic or electrochemical degradation, photocatalysis, ozonation, Fenton process or adsorption (Katsoyiannis et al., 2011; Chahm and Rodrigues, 2017; Capodaglio, 2017; Tarpani and Azapagic, 2018). Adsorption is one of the most promising techniques when applied in current water treatment processes due to its simplicity and low-cost (Ali et al., 2012; Rashed, 2013; Kyzas et al., 2015; Rodriguez-Narvaez et al., 2017; Carmalin and Eder, 2018). Adsorption using activated carbon is highly attractive due to the available high surface area and the combination of well-developed pore structure and surface functional group properties (Li et al., 2002; Dabrowski et al., 2005; Yu et al., 2008). However, this technique has a high cost because only a small percentage of carbons, usually no more than 40%, can be reused after the adsorption process (Wang and Balasubramanian, 2009; Sharma and Wankat, 2010; Marques et al., 2017). To overcome these drawbacks, clay minerals have attracted much

attention because of their high cation exchange capacity (CEC), swelling properties, and high surface areas (Lagally, 2001; Alba et al., 2006; Zadaca et al., 2007; Sánchez-Martín et al., 2008; De Oliveira et al., 2017).

Expandable clay minerals have a marked hydrophilic character caused by the strong hydration of the inorganic counter ions present in the interlayer space. Indeed, they are rarely good adsorbents for hydrophobic organic compounds (Gámiz et al., 2015). One of the strategies to improve the capacity of these clays to adsorb organic contaminants is surfactant loading, which turns clays into organo-clays. Surface activation due to the presence of non-polar alkyl chains, the expansion of interlayer spaces or the hydrophobization are some of the main changes that occur with modification with surfactant cations (Pazos et al., 2012; Pazos et al., 2017; Rodríguez-Narváez et al., 2017; ~~Bujdák~~ Bujdáková et al., 2018; Orta et al., 2018). For example, recent studies have demonstrated the high potential of C_{18}-mica-4 to adsorb organic pollutants such as linear alkylbenzene sulfonates, phenolic compounds, preservatives and other groups of emerging pollutants (Pazos et al., 2017; Martín et al., 2018; Orta et al., 2018). Martín et al. (2018) evaluated the removal of different types of emerging pollutants (perfluoroalkyl compounds, parabens, surfactants and pharmaceutical compounds) from aqueous solution by adsorption onto a high-charge swelling mica (Na-Mica-4) and an organo-functionalized mica (C_{18}-Mica-4). The experiments revealed high adsorption affinity to the C_{18}-Mica-4 for most of the emerging pollutants (14 out of 18 pollutants were effectively removed), while for Na-mica only 3 out of 18 selected pollutants showed high adsorption. A high correlation was observed between the physicochemical properties of selected emerging pollutants (log K_{ow}) and the adsorption onto C_{18}-Mica-4, indicating that in these cases adsorption is mainly due to hydrophobic interactions between the organic compounds and the surfactant alkyl chains

97 of the modified clay.

98 It is well-known that the leading mechanism in the adsorption of organic pollutants by
99 organo-clays will depend, for a given clay mineral, on the properties of the organic
100 modifier and those of the selected solute. So, the goals of this work were to prepare and
101 characterize two functional materials, a natural montmorillonite modified with the cationic
102 octadecylamine (C_{18}-Mt) and a synthetic mica modified with the cationic octadecylamine
103 (C_{18}-mica-4), perform kinetic adsorption studies to optimize the most suitable conditions
104 and to compare and explore their potential uses as adsorbent of waters containing the
105 emerging compound ibuprofen. To the best of our knowledge, the C_{18}-Mt has not been
106 previously evaluated for the adsorption of pharmaceutical compounds.

107

108 **2. Materials and methods**

109 *2.1. Materials and reagents*

110 Mt from Patagonian (Rio Negro, Argentina) supplied by Catiglioni Pes and Co. was used.
111 The chemical composition was $[(Si_{3.83}Al_{0.11})(Al_{1.43}Fe^{3+}_{0.26}Mg_{0.30})O_{10}(OH)_2]$
112 $Na_{0.30}Ca_{0.09}K_{0.01}$, the mineral composition was Na-montmorillonite (>99%) with quartz and
113 feldspars as minor phases (Magnoli et al., 2008) and CEC was 82.5 cmol/kg clay (Gamba et
114 al., 2015).

115 SiO_2 (Sigma Aldrich; CAS no. 112945-52-5, 99.8% purity), $Al(OH)_3$ (Sigma Aldrich; CAS
116 no. 21645-51-2), MgF_2 (Sigma Aldrich; CAS no. 7783-40-6), NaCl (Sigma Aldrich; CAS
117 no. 7647-14-5, ≥99.5% purity) and primary alkylamine octadecylamine salt (CAS no. 124-
118 30-1, ≥99.0% purity) were purchased from Sigma-Aldrich.

119 High Performance Liquid Chromatography grade, acetonitrile and water were supplied by
120 Romil Ltd. (Barcelona, Spain).

Hydrochloric acid, sodium hydroxide and formic acid were obtained from Panreac (Barcelona, Spain). Ammonium formate was purchased from Sigma-Aldrich (Steinheim, Germany). All of them were analytical grade.

High purity standards of ibuprofen was purchased from Dr. Ehrenstorfer (Augsburg, Germany).

Stock standard solution of ibuprofen (1000 mg/L) was prepared in methanol and stored at 4°C. Fresh working solutions at different concentration levels were prepared in water before each experiment.

2.2. Synthesis of the swelling high charged Na-mica-4

Na-mica-4 was synthesized by the NaCl melt method following a procedure described by Alba et al. (2006). Its CEC is 468 cmol/kg and its structural formula is $Na_4[Si_4Al_4]Mg_6O_{20}F_4 \cdot nH_2O$. The starting products employed were SiO_2, $Al(OH)_3$, MgF_2 and NaCl. The reactants were weighed and mixed in an agate mortar until the mixture was homogeneous.

Heat treatments were carried out in a Pt crucible at 900°C during 15 h using a heating rate of 10°C/min. The product was washed with distilled water, and the solid was separated by filtration, dried at room temperature, and then powdered in agate mortar.

2.3. Organo-functionalization of Na-mica-4 and Mt with octadecylamine

The organomica C_{18}-mica-Na and C_{18}-Mt were prepared by a cation-exchange reaction between the Na-mica-4/ Mt and an excess of primary octadecylamine (2 CEC of Na-mica-4/ Mt) (Alba et al., 2011). The primary amines were dissolved in an equivalent amount of HCl (0.1 M) and the resulting mixture was stirred for 3 h at 80°C. The alkylammonium

145 solution was then mixed with 0.6 g of Na-mica-4/ Mt and stirred for 3 h at 80ºC. Deionized
146 water (50 mL at 50ºC) was added and the mixture was stirred for 30 min at 50ºC, and the
147 dispersion was then centrifuged at 8000 rpm for 30 min at 5ºC. The product was dissolved
148 in a hot ethanol:water mixture (1:1) and stirred for 1 h and centrifuged at 8000 rpm for 30
149 min at 5ºC. Finally, the precipitate was left to dry at room temperature.
150
151 *2.5. Characterization methods*
152 *X-ray diffraction* results were obtained in a Bruker D8 Advance A25 diffractometer
153 (Bruker, Germany) in Bragg-Brentano configuration. The detector was a Lynxeye PSD
154 detector (Bruker, Germany) equipped with a copper Kα radiation source (0.15405 nm
155 wavelength). Measurements were taken with a 2θ range between 1° and 70°, a step of
156 0.03°, time per step of 0.1 s, and tube conditions of 40 kV and 30 mA. The diffractometer
157 was calibrated mechanically according to the manufacturer specifications and corundum
158 standard was used to check the resolution in a wide range of angles.
159 The *Zeta potential* was obtained from the mobility of the particles using the Smoluchowski
160 equation (Smoluchowski, 1941). Before and after of adsorption experiments, C_{18}-mica-Na
161 was suspended in water (1 g/L) and the zeta potentials were measured on a Zetasizer
162 Nanosystem system (Malvern Instruments, Southborough, MA). The pH of the solution
163 was measured with Crison GLP 21 pH meter.
164 *Thermal gravimetric analyses* (TGA) were performed on a Q600 STD (TA instruments,
165 USA). The samples were heated from 20°C to 900°C at a heating rate of 10°C/min in a
166 nitrogen atmosphere.
167 *High Performance Liquid Chromatography-tandem mass spectrometry* (HPLC-MS/MS)
168 analyses were performed on an Agilent 1200 series system (Agilent, USA) equipped with a

169 vacuum degasser, a binary pump, an autosampler and a thermostatic column compartment.
170 Separation of ibuprofen was carried out using a HALO C18 (50x4.6 mm i.d.; 2.7 µm)
171 analytical column (Teknokroma, Spain) protected by a HALO C18 (5x4.6 mm 1.d.; 2.7
172 µm) guard column (Teknokroma, Spain). Elution was performed by isocratic conditions
173 with acetonitrile (0.1% formic acid) (80%) and a 10 mM aqueous solution of ammonium
174 formate (0.1% formic acid) (20%), at a flow rate of 0.6 mL min^{-1} with a column
175 temperature of 30°C.
176 A 6410 triple quadrupole (QqQ) mass spectrometer (MS) equipped with an electrospray
177 ionization source (Agilent, USA) was used for detection. Ionization of analytes was carried
178 out using the following settings: MS capillary voltage, 3000 V; flow rate of the drying-gas,
179 9 L/min; drying-gas temperature, 350ºC; and nebulizer pressure was 40 psi. MassHunter
180 software (Agilent, USA) was used for instrument control and data acquisition. Compounds
181 were analysed in multiple reaction monitoring (MRM) mode and monitored in the positive
182 ionization mode. Two MRM transitions were selected for each analyte, one was applied for
183 quantification (251 > 83) and another for confirmation (251 > 129) using a fragmentor of
184 77 V and an energy collision of 8 eV.
185
186 *2.5. Adsorption of ibuprofen*
187 Each batch adsorption test was prepared in a 20 mL vessel, with 20 mg of C_{18}-Mt or C_{18}-
188 mica-Na containing 10 mL of a solution of ibuprofen (10 µg mL^{-1}). The samples were
189 equilibrated for 1 h in an orbitals shaker at 800 rpm at room temperature. A pH of
190 approximately 6.5 remained constant during the adsorption process in all samples. After the
191 contact time, the suspensions were centrifuged at 8000 rpm during 15 min. Solids
192 recovered with maximum ibuprofen adsorption were freeze-dried for further

193 characterization. The supernatants were then filtered through a 0.22 µm nylon filter and a
194 20 µL aliquot was injected into the chromatograph.
195 The parameters affecting ibuprofen adsorption, such as concentration (from 0.5 to 80
196 mg/L), time (from 30 s to 7 days) and sample pH (from 1 to 12) were evaluated and
197 compared. The experiments were run in triplicate. The linearity of the method was studied
198 by analysing standard solutions in triplicate at concentrations ranging from 0.1 µg/mL to
199 10000 µg/mL.
200 The difference in the amount before and after adsorption reveals the amount of adsorbed
201 ibuprofen (q):

202 $$q = (C_i - C_e) \cdot \frac{V}{m} \quad (1)$$

203 where the V (L) is the volume of the solution, m is the weight of the clay (kg), C_i (µmol/L)
204 and C_{eq} (µmol/L) are the concentration of the ibuprofen in initial and final solution,
205 respectively. Control experiments were performed without organoclays and indicated the
206 negligible loss of ibuprofen by volatilization or by adsorption on the glass tubes. Also,
207 procedural blanks (samples without ibuprofen) were injected to monitor background
208 contamination. Blanks were processed in the same way as the samples and injected into the
209 HPLC-MS/MS system. No quantifiable amounts of ibuprofen were detected.
210 The adsorption percentage was calculated as follows:

211 $$\%adsorption = \frac{(C_i - C_e)}{C_i} \cdot 100 \quad (2)$$

212 The adsorbent performance was determined by adjustment of the experimental isotherms to
213 Langmuir, Freundlich and Dubinin-Radushkevitch (DR) mathematical model (Marco-
214 Brown et al., 2014). The Langmuir model is described by the following equation:

215 $$q = \frac{q_{max} K_L C_e}{1 + (C_e K_L)} \quad (3)$$

where, q_{max} is the maximum amount adsorbed within a monolayer (μmol/g), and K_L (L/μmol) is the Langmuir dissociation constant, which is related to the adsorption energy.

The Freundlich model is described by equation 4:

$$q = K_F C_e^{\,1/n} \quad (4)$$

where, K_F (L/μmol) is the Freundlich constant, which is related to the affinity of the adsorbent to the adsorbate, and 1/n is a dimensionless parameter, which indicates how adsorption varies as a function of the concentration.

The DR model is more general than the Langmuir model because the former does not assume a homogeneous surface or a constant adsorption potential. This model is described by the following equation:

$$q = q_{max} e^{-K_{DR}\varepsilon^2} \quad (5)$$

where, K_{DR} (mol^2/J^2) is a DR constant and ε (J/mol) is a Polanyi potential, which is related to C_e by the following equation:

$$\varepsilon = RT\ ln\left(1 + \frac{1}{C_e}\right) \quad (6)$$

where, R is the gas constant and T is the temperature in Kelvin. K_{DR} is related to the mean free energy of adsorption per mole of adsorbate (E, kJ/mol) according to equation 7.

$$E = (2K_{DR})^{-1/2} \quad (7)$$

The following mathematical models were employed for the kinetic analysis: pseudo first order (PFO), pseudo second order (PSO), intra-particle diffusion (IDM), and Elovich models (equations 8-11, respectively) (Marco-Brown et al., 2014).

$$ln\ (q_e - q_t) = ln\ q_e - k_1 t \quad (8)$$

$$\frac{t}{q_t} = \frac{1}{k_2 q_e^2} + \frac{t}{q_e} \quad (9)$$

$$q_t = k_{id}\sqrt{t} + C \quad (10)$$

$$\frac{dq_t}{dt} = \alpha\, exp(-\beta q_t) \quad (11)$$

where q_e and q_t are the amount of ibuprofen adsorbed at equilibrium and at time t, respectively; k_1, k_2 and k_{id} are the rate constants for PFO, PSO, and IDM models, respectively. C is a constant, and α and β are the Elovich coefficients.

To determine the goodness of the fit of the model to the experimental data, in addition to the value of R^2, the percentage standard deviation [Δq (%)] was calculated from the following equation:

$$\Delta q(\%) = \sqrt{\frac{\sum[\frac{q_t - q_t^{cal}}{q_t}]^2}{n-1}}\; x\; 100 \quad (12)$$

where, q_t^{cal} is the calculated amount of ibuprofen adsorbed and n is the number of measurements.

3. Results and discussion

3.1. Characterization of C_{18}-Mt and C_{18}-mica-4

X-ray diffraction: Le Bail analysis (Le Bail, 2005) was conducted using the TOPAS 6 software (Bruker, 2017). It is a profile fitting technique used to extract precise information about the position, intensity, width, and shape of each individual peak in a diffraction pattern (Orta et al., 2018, Martín et al., 2018). The values of the goodness of fit (GOF) of the adjustments were checked to obtain values close to unity. At the same time values of residual factors R_{wp} and R_{Bragg} were obtained. In the reported results these values were generally small indicating coherent data (Young, 1993).

GOF value obtained from the Le Bail fitting for C_{18}-mica-4 was 2.27, and R_{wp} and R_{Bragg} were 8.61 and 0.611, respectively. The structure used was triclinic in space group P1 (Orta et al., 2018) and the lattice parameters were: a = 50.040(12) Å, b = 9.902(3) Å, c = 9.787(3) Å, α = 89.43(2) °, β = 86.69(2) °, γ = 89.24(2) °, and d = 49.95285 Å and 2Θ = 1.76713° for the (001) plane. GOF, Rwp and RBragg values were 1.98, 7.96 and 0.611, respectively, after the adsorption process of ibuprofen. The lattice parameters were: a = 50.093(13) Å, b = 9.731(2) Å, c = 9.943(2) Å, α = 89.057(17) °, β = 89.20(2) °, γ = 86.985(18) °, and d= 50.01913 Å and 2Θ = 1.76479° for the (001) plane.

The C_{18}-Mt corresponds with a triclinic structure and X-ray diffraction characterization tests showed an increase from 20.96 Å (4.21º 2Θ corresponding to C_{18}-Mt, black line in Figure 1a) to 21.65 Å (4.08º 2Θ corresponding to C_{18}-Mt after the adsorption, red line in Figure 1a) in the interlayer space. The difference causes a change in the tilt angle (α) between the alkylammonium axis and the solid surface after adsorption of ibuprofen in the interlayer space, which increased from 15.18° to 16.10° (Alba et al., 2011).

XRD characterization tests showed a slightly increase from 49.95 Å (1.767º 2Θ corresponding to C_{18}-mica-4, black line in Figure 1b) to 50.02 Å (1.765º 2Θ corresponding to C_{18}-mica-4 after the adsorption, red line in Figure 1b) in the interlayer space. This difference is seen in Figure 1b that shows the diffraction diagrams of the main peaks for pure C_{18}-mica-4 and C_{18}-mica-4 after adsorption assay. The difference causes a change in the tilt angle (α) between the alkylammonium axis and the solid surface after adsorption of ibuprofen in the interlayer space, which increased from 66.70° to 66.93° (Alba et al., 2011).

Zeta Potential: The external surface charge of C_{18}-Mt and C_{18}-mica-4 before and after the adsorption assays was studied at pH~6.5. The Zeta potential values were 46.78 ± 0.94 mV and 34.90 ± 1.04 mV, respectively for the C_{18}-Mt, and 52.92 ± 1.10 mV and 24.69 ± 0.95

mV respectively for the C_{18}-mica-4. These different values in the external surface charge of C_{18}-Mt and C_{18}-mica-4 indicate that adsorption of ibuprofen could also occur in the surface. Figure S1 shows the effect of pH on the zeta potential value for C_{18}-Mt (a) and C_{18}-mica-4 (b) and Zeta Potential value at to pH 6.5 of C_{18}-Mt-Ibuprofen (a) and C_{18}-mica-4-Ibuprofen (b).

Thermal Gravimetric analyses: Figure 2a shows the results of the TGA obtained for C_{18}-Mt before and after the adsorption assays. The thermal decomposition of C_{18}-Mt and C_{18}-Mt with ibuprofen adsorbed was analyzed at three temperature ranges. The low mass loss until 170ºC is assigned to the evaporation of the water retained in the interstices of the clays (Alba et al., 2011), the amount of water in the interlaminar space is low when it has been displaced to a large extent by the surfactant, this loss is slightly lower in C_{18}-Mt-ibuprofen, when the drug occupies part of the interlayer space. Mass loss between approximately 170 and 550ºC is associated with dehydroxylation of de Mt. Finally, the mass loss between 600 y 850ºC is attributed to the release of carbonaceous residues from the interlayer space (Hedley et al., 2007), the loss is major in C_{18}-Mt after adsorption due to the ibuprofen retained.

Figure 2b shows the results of the TGA obtained for C_{18}-mica-4 before and after the adsorption assays. Both materials showed a slight decrease of weight at about 170°C due to the low amount of water present in it. A mass loss of up to 50% and up to 65% to the C_{18}-mica-4 and C_{18}-mica-4 with ibuprofen adsorbed, respectively, occurred between 170°C and 450 °C, primarily due to degradation of ibuprofen and the alkylammonium chains in the interlayer space (Orta et al. 2018, Martín ~~Martin~~ et al. 2018).

The greater weight loss of Na-mica-4 compared to Mt, can be explained by the greater amount of surfactant retained due to its increased CEC. Figure S2 shows the processes that

cause a decrease in the heat flow that corresponds to an endothermic peak as heat is required in the process of evaporation of the water retained in the interstices. The exothermic and endothermic shoulders from 350 °C to 470 °C correspond to the degradation of alkylammonium chains and the release of carbonaceous waste from the interlayer space corresponds to an endothermic process.

3.2. Adsorption of ibuprofen by C_{18}-Mt and C_{18}-mica-4

The adsorption experiments showed that the extent of ibuprofen retention was subjected to the structure and features of each organoclay (Figure 3). Experimental data of ibuprofen adsorption on C_{18}-Mt and C_{18}-mica-4 loaded samples is shown in Figure 3 a and b, respectively, as the function of the equilibrium adsorption capacity of ibuprofen (q) versus the equilibrium concentration of ibuprofen (C_e) in the testing solutions. The % of C_{18}-Mt adsorbed remained unaltered (> 99.9%) in the range 0.5-80 mg/L. However, in case of C_{18}-mica-4 the adsorption rates of 99.9% were not affected by the ibuprofen concentration in the range 0.5-10 mg/L while this % decrease to 67% at 80 mg/L (Figure 3b top).

In case of C_{18}-Mt, the shapes of the isotherms showed L behaviour according to Giles classification (Giles et al., 1960). This is characteristic of systems where the adsorbate presents high affinity towards the adsorbent, and therefore indicates that no strong competition of the solvent takes place for the active sites of adsorption (Mestre et al., 2009). These pattern and adsorption capacities are in agreement with data from the literature of aqueous ibuprofen solution in other materials such as active carbon (Mestre et al., 2009; Bahamon et al., 2017).

The sigmoidal isotherm shape is exhibited by C_{18}-mica-4. This adsorption isotherm type is due to two mechanisms: one in which the sorption is favoured by the attractive forces

331 solute-solute and a cooperative sorption occurs, and another, in which the sorption can be
332 inhibited by a competitive reaction in the solution (Pazos et al., 2017). Ibuprofen could be
333 adsorbed into covering the surface, allowing other molecules being more readily adsorbed,
334 in a model of cooperative adsorption. So, it is evident that the characteristics of the
335 adsorbent material dictate the efficiency of the adsorption process (Rodríguez-Narvaez et
336 al., 2017).
337 The fit correlation coefficients (R^2) and the adjustment parameters obtained from
338 Langmuir, Freundlich and DR equations are shown in Table 1. The Langmuir and
339 Freundlich models gave a better fit for C_{18}-Mt and C_{18}-mica-4, respectively on the basis of
340 the correlation coefficient values (R^2). In both materials, the Freundlich parameter n
341 suggests when 1/n is between 0.1 and 1 a favourable adsorption process (de Oliveira et al.,
342 2017). Regarding the DR model, the free energy E of adsorption (kJ/mol) with Eq. (7)
343 provides information about adsorption mechanism. If $E < 8$ kJ/mol, the adsorption process
344 follows a molecular interactional mechanism preferentially, while for $E > 8$ kJ/mol ion-
345 exchange is envisaged. E values showed in Table 1 could indicate an ionic exchange
346 between negatively charged ibuprofen and inorganic cations in the free sites of Mt and Na-
347 mica-4 (not occupied by organic cations) could be the dominant adsorption mechanism.
348
349 *3.3. Adsorption kinetic*
350 The kinetic behaviours of C_{18}-Mt and C_{18}-mica-4 were examined and compared in order to
351 get a comparison of the relative kinetic performance of these adsorbents for ibuprofen
352 removal. The experiments were made using an ibuprofen solution at $C_i = 10$ mg/L. Figure 4
353 a, b shows the kinetic data obtained. According to the results, equilibrium was
354 approximately reached after 5 and 60 minutes for C_{18}-Mt and C_{18}-mica-4, respectively, to

355 remove ibuprofen (>99%) from aqueous solution. In addition, as can be seen from Figure 4,
356 after adsorption, ibuprofen remained retained into the materials at least seven days after the
357 assay.
358 In order to examine the rate controlling mechanism of adsorption process, the PFO, PSO,
359 IDM and Elovich models were evaluated to fit the experimental data. The parameters of
360 each equation as well as R^2 and Δq (%) are shown in Table 2, and the resulting curves are
361 shown in Figure 4 a, b. Data obtained from kinetic studies for both materials is fitted to the
362 PSO model better than the others ($R^2 > 0.993$), although the Elovich models yielded lower
363 Δq (%) values. The results also pointed out that C_{18}-Mt has the highest rate constants, k_2,
364 obtained by the PSO kinetic model. This model describes a chemisorption mechanism and
365 is based on the adsorption capacity of the solid phase and on the assumption that the initial
366 concentration of adsorbate is comparable to the adsorption sites available in the adsorbent.
367
368 *3.4. Influence of the pH on the ibuprofen adsorption*
369 The pH of the solution has been identified as the most important variable affecting pollutant
370 adsorption onto adsorbents (Zhang et al., 2015; de Oliveira et al., 2017). The adsorption of
371 compound with charged groups onto the adsorbent surface is influenced by the surface
372 charge on the adsorbent, which is influenced by the pH of the solution. The adsorption of
373 ibuprofen onto both materials as a function of pH was investigated for pH values ranging
374 from 1 to 12 with an initial concentration of ibuprofen of 10 mg/L. Figure 5 shows the
375 effect of the sample pH.
376 High % adsorption (>99.9%) was obtained for pH range 4–9. The adsorption efficiency was
377 found to be highly dependent on the proton concentration of the solution. When the pH
378 goes down of 4 the % adsorption significantly decreased from 99.9% to 80.7% and 71.4%

379 for C_{18}-Mt and C_{18}-mica-4, respectively. Ibuprofen is a weak acid, and pH has a significant
380 effect on the degree of ionization and charge. Ibuprofen became negatively charged as the
381 pH rises above 4. The effect of pH can be explained by considering the surface charge of
382 the organoclays. On the other hand, the adsorption rates of both organoclays were affected
383 by extremely acidic (pH 1) and basic (pH 12) pH values.
384 These results suggest that the pH value of the ibuprofen solution plays an important role in
385 the whole adsorption process, particularly in the adsorption capacity. Nevertheless, as
386 adsorption rates of both organoclays were not affected by the sample pH in the range from
387 4 to 9, no sample pH adjustment is necessary to remove the target compound from water
388 samples. Further studies using sophisticated techniques should be carried out to answer the
389 binding mechanisms of ibuprofen on the adsorbents (Tan et al., 2014).
390

391 **4. Conclusions**

392 For the first time, two organoclays, a natural Mt and synthetic Na-mica-4 modified with the
393 cationic octadecylamine (C_{18}-Mt and C_{18}-mica-4, respectively) were evaluated and
394 compared for the adsorption of ibuprofen in water samples. The characterization
395 experiments showed the entrance of ibuprofen in both materials. Results of X-ray
396 diffraction and Zeta potential analysis indicate that the adsorption of ibuprofen occurs in
397 the interlayer space and surface in both cases. Differences between both materials were
398 observed regarding the adsorption mechanisms. Ibuprofen adsorption onto C_{18}-Mt was well
399 described by the Langmuir model while C_{18}-mica-4 fitted better the Freundlich model.
400 Regarding the equilibrium time, ibuprofen adsorption was slightly faster in C_{18}-Mt (< 5
401 min) than in C_{18}-mica-4 (< 60 min). The better kinetic fit model on both materials to the
402 PSO model indicated a chemisorption mechanism.

403 The reported data represents a promising area of research in the field of wastewater
404 treatment technologies. The expansion capacity after their organo-functionalization
405 together with their easy availability and relatively low cost is promising developments for a
406 bright future in the field of adsorption technology. Further studies should be carried out to
407 extend the use of these promising materials in wastewater samples and to answer the
408 binding mechanisms of ibuprofen on the adsorbents.
409
410 **Acknowledgement**
411 This work was supported by the Spanish Ministry of Economy, Industry and
412 Competitiveness (Project No. CTM2017-82778-R) and by the University of Seville through
413 the *VI Plan Propio de Investigación*. The authors are grateful to the X-ray Laboratory, and
414 Functional Characterization Services of the *Centro de Investigación Tecnología e*
415 *Innovación de la Universidad de Sevilla* (CITIUS).
416
417 **References**
418 Alba, M.D., Castro, M.A., Naranjo, M., Pavón, E., 2006. Hydrothermal reactivity of Na-n-
419 Micas (n = 2, 3, 4). Chem. Mater. 18, 2867–2872.
420 Alba, M.D., Castro, M.A., Orta, M.M., Pavón, E., Pazos M.C. and Valencia J.S., 2011.
421 Formation of organo-highly charged mica. Langmuir 27 (16), 9711–9718.
422 Ali, I., Asim, M., Khan, T.A., 2012. Low cost adsorbents for the removal of organic
423 pollutants from wastewater. J. Environ. Manag. 113, 170-183.
424 Bahamon, D., Carro, L., Guri, S., Vega, L.F., 2017. Computational study
425 of ibuprofen removal from water by adsorption in realistic activated carbons. J.
426 Colloid Interface Sci. 498, 323-334.

427 Bujdáková, H., Bujdáková, V., Májeková-Koščová, H., Gaálová, B., Bizovská, V., Boháč,
428 P., Bujdák, J., 2018. Antimicrobial activity of organoclays based on quaternary
429 alkylammonium and alkylphosphonium surfactants and montmorillonite. Appl. Clay
430 Sci. 158, 21–28.
431 Bruker, 2017. Bruker AXS GmbH, Karlsruhe, Germany Search PubMed.
432 Capodaglio, A.G., 2017 High-energy oxidation process: an efficient alternative for
433 wastewater organic contaminants removal. Clean Technol. Environ. Pol. 19(8), 1995–
434 2006.
435 Carmalin, S.A., Eder, C.L., 2018. Removal of emerging contaminants from the
436 environment by adsorption. Ecotoxicol. Environ. Saf. 150, 1–17.
437 Carvalho, A.P., Mestre, A.S., Andrade, M., Ania, C.O., Ibuprofen in the aquatic
438 environment: Occurrence, ecotoxicity and water remediation technologies. In:
439 Ibuprofen: Clinical Pharmacology, Medical Uses and Adverse Effects. Edition: 1st,
440 Chapter: 1, Publisher: Nova Science Publishers, Editors: Wilton C. Carter, Brant R.
441 Brown, 2013; pp.1-84.
442 Chahm, T., Rodrigues, C.A., 2017. Removal of ibuprofen from aqueous solutions using O-
443 carboxymethyl-N-laurylchitosan/γ-Fe2O3. Environ. Nanotechnol. Monit. Manag. 7,
444 139-148.
445 Dabrowski, A., Podkoscielny, P., Hubicki, Z., Barczak, M., 2205. Adsorption of phenolic
446 compounds by activated carbon – a critical review. Chemosphere 58, 1049–1070.
447 De Oliveira, T., Guégan, R., Thiebault T., Le Milbeau C., Muller, F., Teixeira, V.,
448 Giovanela, M., Boussafir. M., 2017. Adsorption of diclofenac onto organoclays:
449 Effects of surfactant and environmental (pH and temperature) conditions. J. Haz. Mat.
450 323, 558–566.

451 Directive, 2013. 2013/39/EU of the European Parliament and of the Council of 12 August
452 2013 amending Directives 2000/60/EC and 2008/105/EC as regards priority
453 substances in the field of water policy. Off. J. Eur. Union L226, 1e17.
454 Gamba, M., Flores, F.M., Madejová, J., Sánchez, R.M.T., 2015. Comparison of imazalil
455 removal onto montmorillonite and nanomontmorillonite and adsorption surface sites
456 involved: An approach for agricultural wastewater treatment. Ind. Eng. Chem. Res.
457 54 (5), 1529-1538.
458 Gámiz, B., Hermosín, M.C., Cornejo, J., Celis, R., 2015. Hexadimethrine-montmorillonite
459 nanocomposite: Characterization and application as a pesticide adsorbent. Appl. Surf.
460 Sci. 332, 606–613.
461 Giles, C.H., Macewan, T.H., Nakhwa, S.N., Smith, D.J., 1960. Studies in adsorption. Part
462 XI. A system of classification of solution adsorption isotherms, and its use in
463 diagnosis of adsorption mechanisms and in measurement of specific surface areas of
464 solids. J. Chem. Soc. 786, 3973–3993.
465 Hedley, C.B., Yuan, G., Theng, B.K.G., 2007. Thermal analysis of ~~os~~ montmorillonites
466 modified with quaternary phosphonium and ammonium surfactants. App. Clay Sci.
467 35, 180-188.
468 Katsoyiannis, I.A., Canonica, S., Gunten, U., 2011. Efficiency and energy requirements for
469 the transformation of organic micropollutants by ozone, O_3/H_2O_2 and UV/H_2O_2.
470 Water Res. 45, 3811-22.
471 Kyzas, G.Z., Fu, J., Lazaridis, N.K., Bikiaris, D.N., Matis, K.A., 2015. New approaches on
472 the removal of pharmaceuticals from wastewaters with adsorbent materials. J. Mol.
473 Liquids, 209, 87-93.

474 Lagally, G., 2001. Pesticides-clay interactions and formulations. App. Clay Sci. 18, 205–
475 209.
476 Le Bail, A., 2005. Whole powder pattern decomposition methods and applications: a
477 retrospection. Powder Diffr. 20, 316.
478 Li, L., Quinlivan, P.A., Knappe, D.R.U., 2002. Effects of activated carbon surface
479 chemistry and pore structure on the adsorption of organic contaminants from aqueous
480 solution. Carbon 40, 2085–2100.
481 Loraine, G., Pettigrove, M., 2006. Seasonal variations in concentrations of pharmaceuticals
482 and personal care products in drinking water and reclaimed wastewater in southern
483 California. Environ. Sci. Technol. 40, 687–695.
484 Magnoli, A.P., Tallone, L., Rosa, C.A.R., Dalcero, A.M., Chiacchiera, S.M., Torres
485 Sanchez, R.M., 2008. Commercial bentonites as detoxifier of broiler feed
486 contaminated with aflatoxin. Appl. Surf. Sci. 40 (1-4), 63-71.
487 Marco-Brown, J.L., Areco, M.M., Torres Sánchez, R.M., dos Santos Alfonso, M., 2014.
488 Adsorption of picloram herbicide on montmorillonite: Kinetic and equilibrium
489 studies. Colloids and Surfaces A: Physicochem. Eng. Aspects 449, 121-128
490 Marques, S.C.R., Marcuzzo, J.M., Baldan, M.R., Mestre, A.S., Carvalho, A.P., 2017.
491 Pharmaceuticals removal by activated carbons: role of morphology on cyclic thermal
492 regeneration. Chem. Eng. J. 321, 233–244.
493 Martín, J., Camacho-Muñoz, D., Santos, J.L., Aparicio, I., Alonso, E., 2011. Monitoring of
494 pharmaceutically active compounds on the Guadalquivir River basin (Spain):
495 occurrence and risk assessment. J. Environ. Monit., 2011, 2042-2049.
496 Martín, J., Orta, M.M., Medina-Carrasco, S., Santos, J.L., Aparicio, I., Alonso, E., 2018.
497 Removal of priority and emerging pollutants from aqueous media by adsorption onto

498 synthetic organo-funtionalized high-charge swelling micas. Environ. Res. 164, 488–
499 494.
500 Mestre, A.S., Pires, J., Nogueira, J.M.F., Parra, J.B., Carvalho, A.P., Ania, C.O., 2009.
501 Waste- derived activated carbons for removal of ibuprofen from solution: role of
502 surface chemistry and pore structure, Biores. Technol. 100, 1720–1726.
503 Mompelat, S., Le Bot, B., Thomas, O., 2009. Occurrence and fate of pharmaceutical
504 products and by-products, from resource to drinking water. Environ. Int. 35, 803–
505 814.
506 Orta, M.M., Martín J., Medina-Carrasco S., Santos J.L., Aparicio I., Alonso, E., 2018.
507 Novel synthetic clays for the adsorption of surfactants from aqueous media. J.
508 Environ. Manag. 206, 357-366.
509 Pazos, M.C., Castro M.A., Cota A., Osuna F.J., Pavón E., Alba M.D., 2017. New insights
510 into surface-functionalized swelling high charged micas: Their adsorption
511 performance for non-ionic organic pollutants. J. Ind. Eng. Chem. 52, 179-186.
512 Pazos, M.C., Castro, M.A., Orta, M.M., Pavón, E., Valencia Rios, J.S., Alba, M.D., 2012.
513 Synthetic High-Charge Organomica: Effect of the Layer Charge and Alkyl Chain
514 Length on the Structure of the Adsorbed Surfactants. Langmuir 28, 7325-7332.
515 Rashed, M.N., 2013. Adsorption technique for the removal of organic pollutants from water
516 and wastewater. In Rashed, M.N., (Ed.), Organic pollutants – monitoring, risk and
517 treatment. Rijeka, Croatia: InTech., pp. 167–194.
518 Rodriguez-Narváez, O.M., Peralta-Hernandez, J.M., Goonetilleke, A., Bandala, E.R., 2017.
519 Treatment technologies for emerging contaminants in water: A review. Chem. Eng.
520 J. 323, 361–380.

521 Sánchez-Martín, M.J., Dorado, M.C., del Hoyo, C., Rodríguez-Cruz, M.S., 2008. Influence
522 of clay mineral structure and surfactant nature on the adsorption capacity of
523 surfactants by clays. J. Hazard. Mater. 150, 115-123.
524 Sharma, P.K., Wankat, P.C., 2010. Solvent recovery by steamless temperature swing
525 carbon adsorption processes. Ind. Eng. Chem. Res. 49, 11602–11613.
526 Sousa, J.C.G., Ribeiro, A.R., Barbosa, M.O., Pereira, M.F.R., Silva, A.M.T., 2018. A
527 review on environmental monitoring of water organic pollutants identified by EU
528 guidelines. J. Haz. Mat. 344, 146–162.
529 Smoluchowski, R., 1941. Anisotropy of the electronic work funtion of metals. Phys. Rev.
530 60, 661-674.
531 Tan, D., Yuan, P., Annabi-Bergaya, F., Liu, D., Wang, L., Liu, H., He, H. 2014. Loading
532 and in vitro release of ibuprofen in tubular halloysite. App. Clay Sci., 96, 50 –55.
533 Tarpani, R.R.Z., Azapagic, A., 2018. Life cycle environmental impacts of advanced
534 wastewater treatment techniques for removal of pharmaceuticals and personal care
535 products (PPCPs). J. Environ. Manag. 215, 258-272.
536 Tran, N.H., Reinhard, M., Gin, K.Y.-H., 2018. Occurrence and fate
537 of emerging contaminants in municipal wastewater treatment plants from different
538 geographical regions-a review. Water Res. 133, 182-207.
539 Vieno, N.M., Tuhkanen, T., Kronberg, L., 2005. Seasonal variation in the occurrence of
540 pharmaceuticals in effluents from a sewage treatment plant and in the recipient water.
541 Environ. Sci. Technol. 39, 8220–8226.
542 Wang, L., Balasubramanian, N., 2009. Electrochemical regeneration of granular activated
543 carbon saturated with organic compounds. Chem. Eng. J. 155, 763–768.
544

545 Wilkinson, J., Hooda, P.S., Barker, J., Barton, S., Swinden, J., 2017. Occurrence, fate and
546 transformation of emerging contaminants in water: An overarching review of the
547 field. Environ. Pollut. 231, 954-970.
548 Yang, Y., Ok, Y.S., Kim, K.-H., Kwon, E.E., Tsang, Y.F., 2017. Occurrences and removal
549 of pharmaceuticals and personal care products (PPCPs) in drinking water and
550 water/sewage treatment plants: A review. Sci. Total Environ. 596–597, 303-320.
551 Young, R.A. (Ed.), 1993. The Rietveld Method; IUCr Monographs on Crystallography No
552 5. Oxford University Press, New York.
553 Yu, Z., Peldszus, S., Huck, P.M., 2008. Adsorption characteristics of selected
554 pharmaceuticals and an endocrine disrupting compound–Naproxen, carbamazepine
555 and nonylphenol–on activated carbon. Water Res. 42, 2873– 82.
556 Zadaka, D., Mishael, Y.G., Polubesova, T., Serban, C., Nir, S., 2007. Modified silicates and
557 porous glass as adsorbents for removal of organic pollutants from water and
558 comparison with activated carbon. Appl. Clay Sci. 36, 174-181.
559 Zhang, L., Zhang, B., Wu, T., Sun, D., Li Y., 2015. Adsorption behavior and mechanism of
560 chlorophenols onto organoclays in aqueous solution. Colloids Surf. A: Physicochem.
561 Eng. Aspects 484, 118–129.
562
563

Graphical Abstract

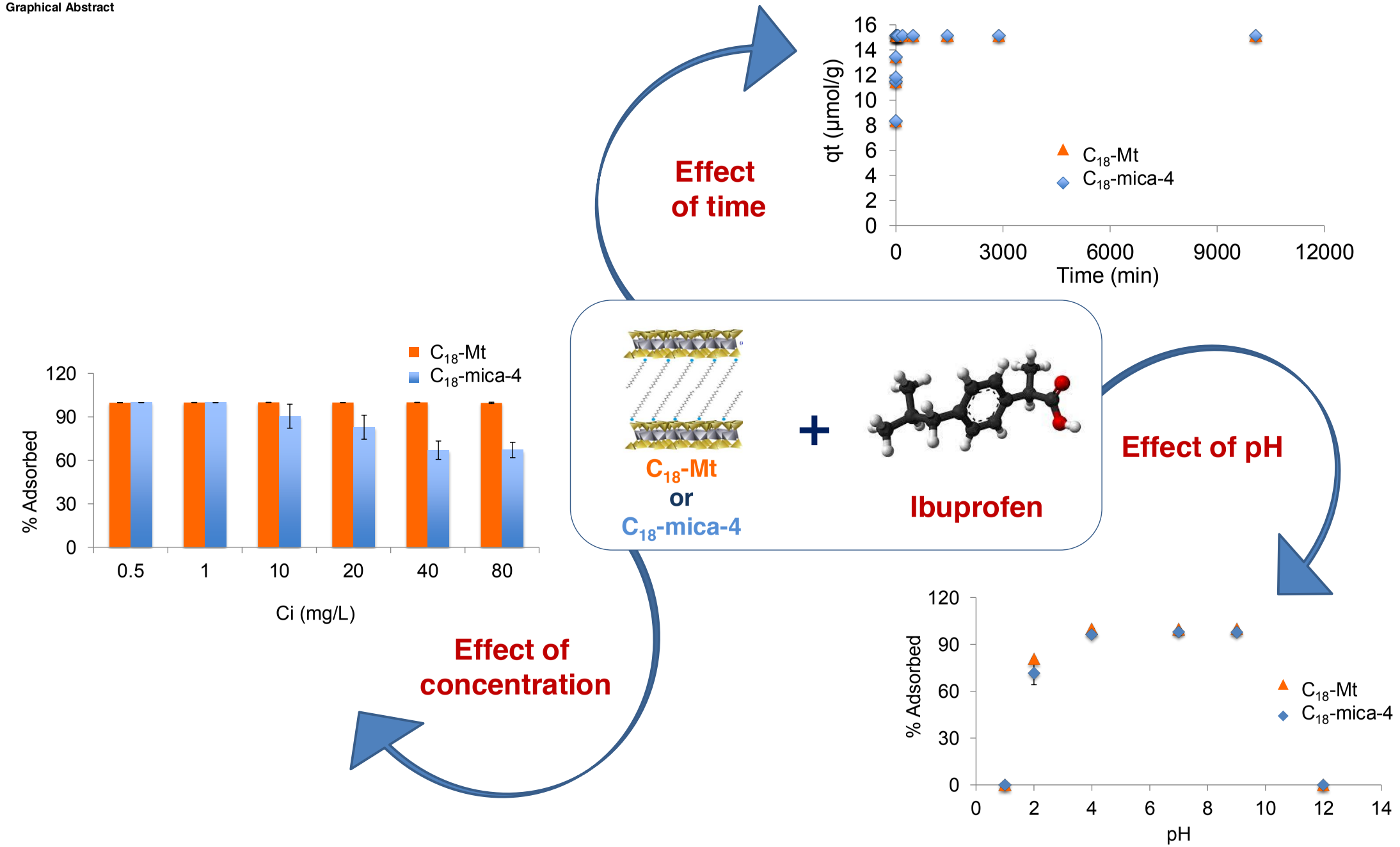

Highlights

- C_{18}-Mt and C_{18}-Mica-4 represent novel adsorbents of ibuprofen from aqueous solutions.
- Results of X-ray diffraction and Zeta potential analysis indicate that the adsorption of ibuprofen occurs in the interlayer space and surface.
- The adsorption equilibrium is faster in C_{18}-Mt (< 5 min) than in C_{18}-mica-4 (<60 min).
- Ibuprofen adsorption onto C_{18}-Mt is well described by the Langmuir model while C_{18}-mica-4 is better fit by the Freundlich model.
- The better kinetic fit model on both materials to the PSO model indicates a chemisorption mechanism.

Table 1
Click here to download Table: Table 1_corrected.docx

Table 1. Langmuir, Freundlich and DR parameters for ibuprofen adsorption on C_{18}-Mt and C_{18}-mica-4.

Model	Parameter	C_{18}-Mt	C_{18}-mica-4
Langmuir	q_{max} (µmol/g)	2.0E+05	7.5E+04
	K_L (L/(µmol)	11.60	0.29
	R^2	0.9975	0.9679
	Δq (%)	23.4	59.1
Freundlich	K_F(L/g)	1.8E+05	1.5E+04
	1/n	0.37	0.45
	R^2	0.9292	0.9938
	Δq (%)	21.5	13.8
DR	q_{max} (µmol/g)	1.6E+06	3.8E+05
	KDR (mol^2/J)	1.9E-09	2.6E-09
	E (KJ/mol)	16.2	14.0
	R^2	0.9418	0.9871
	Δq (%)	23.4	55.4

Table 2
Click here to download Table: Table 2.docx

Table 2. Kinetic parameters of ibuprofen adsorption on C_{18}-Mt and C_{18}-mica-4.

Model	Parameter	C_{18}-Mt	C_{18}-mica-4
	q_e (μmol/g)	15.1 ± 0.1	15.1 ± 0.1
PFO	q_e cal (μmol/g)	6.2 ± 0.8	7.4 ± 0.7
	k_1 (1/min)	0.95 ± 0.05	0.027 ± 0.004
	R^2	0.9901	0.8688
	Δq (%)	47.5	71.7
PSO	q_e cal (μmol/g)	15.6 ± 0.3	13.4 ± 0.4
	k_2 (g/μmol·min)	0.40 ± 0.10	0.05 ± 0.02
	R^2	0.9991	0.9933
	Δq (%)	10.3	31.6
IDM	k_i (μmol/g·$min^{1/2}$)	3.12 ± 0.87	1.01 ± 0.18
	C (μmol/g)	8.86 ± 1.05	6.53 ± 0.68
	R^2	0.8101	0.8149
	Δq (%)	9.5	18.3
Elovich	α (μmol/g·min)	2977 ± 2382	895 ± 462
	β (g/μmol)	0.58 ± 0.06	0.83 ± 0.06
	R^2	0.9683	0.9585
	Δq (%)	2.4	7.3

Figure caption.rev
Click here to download Figure: Figure Caption.rev.docx

Figure 1. a) Experimental diffractograms obtained for C_{18}-Mt and C_{18}-Mt after the adsorption assay of ibuprofen. b) Experimental diffractograms obtained for C_{18}-mica-4 and C_{18}-mica-4 after the adsorption assay of ibuprofen.

Figure 2. Thermal gravimetric analysis before and after adsorption of ibuprofen for C_{18}-Mt (a) and C_{18}-mica-4 (b).

Figure 3. Langmuir, Freundlich and DR models of ibuprofen adsorption on C_{18}-Mt (a) and C_{18}-mica-4 (b).

Figure 4. Kinetic models of ibuprofen adsorption on C_{18}-Mt (a) and C_{18}-mica-4 (b).

Figure 5. Effect of pH on ibuprofen adsorption on C_{18}-Mt (a) and C_{18}-mica-4 (b) (n=3).

Figure 1.rev

Click here to download Figure: Figure 1_revised.pdf

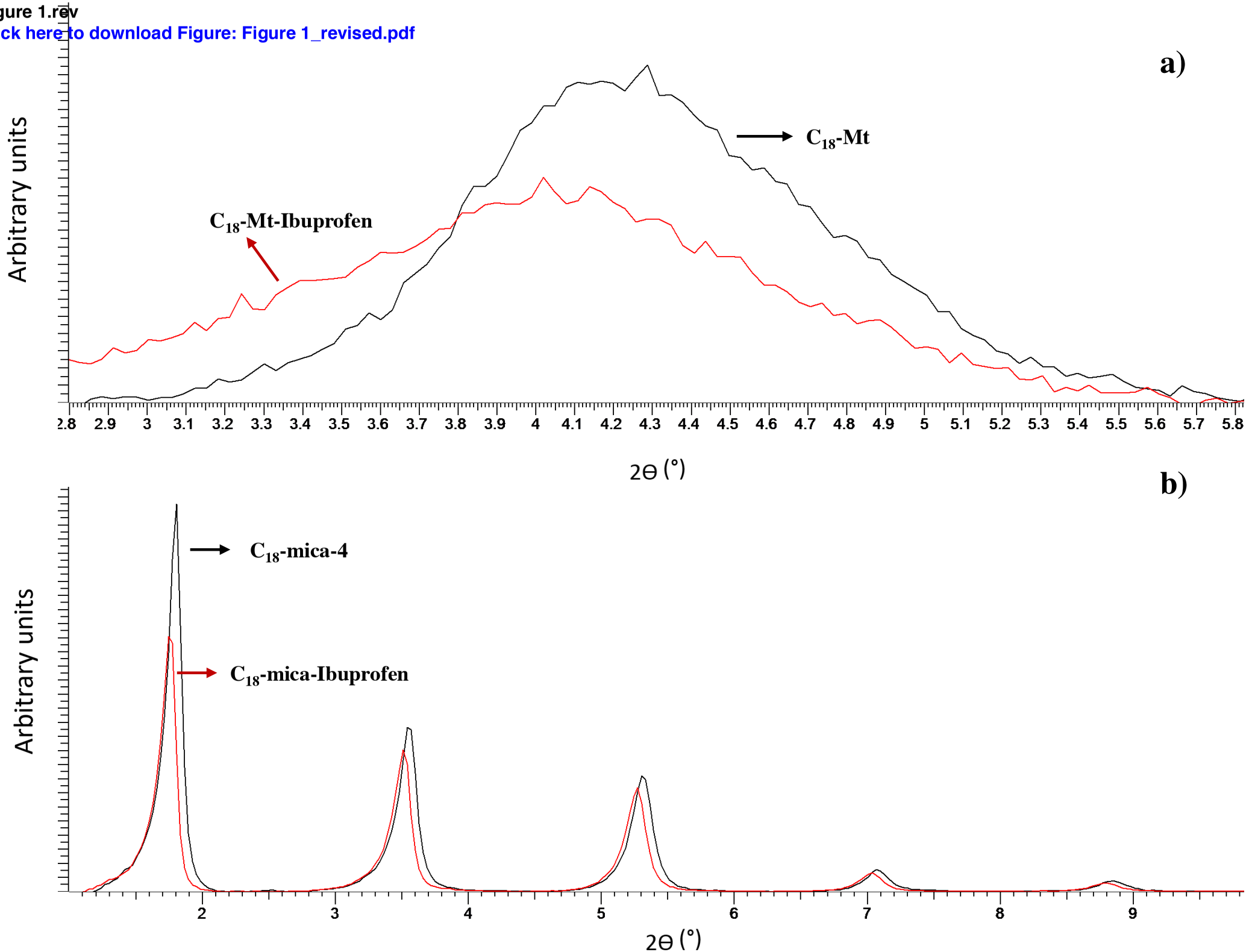

Figure 2

Click here to download Figure: Figure 2.pptx

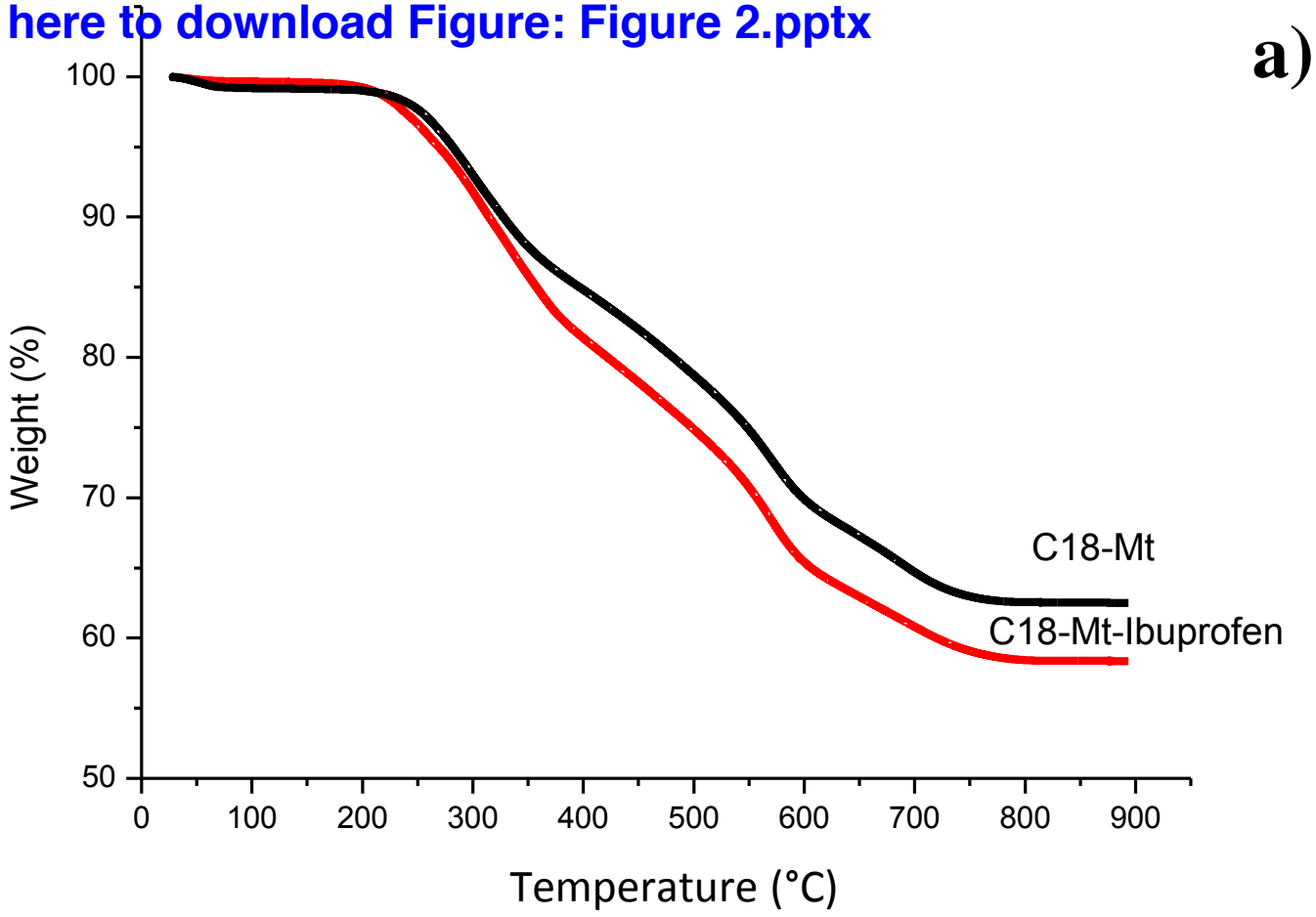

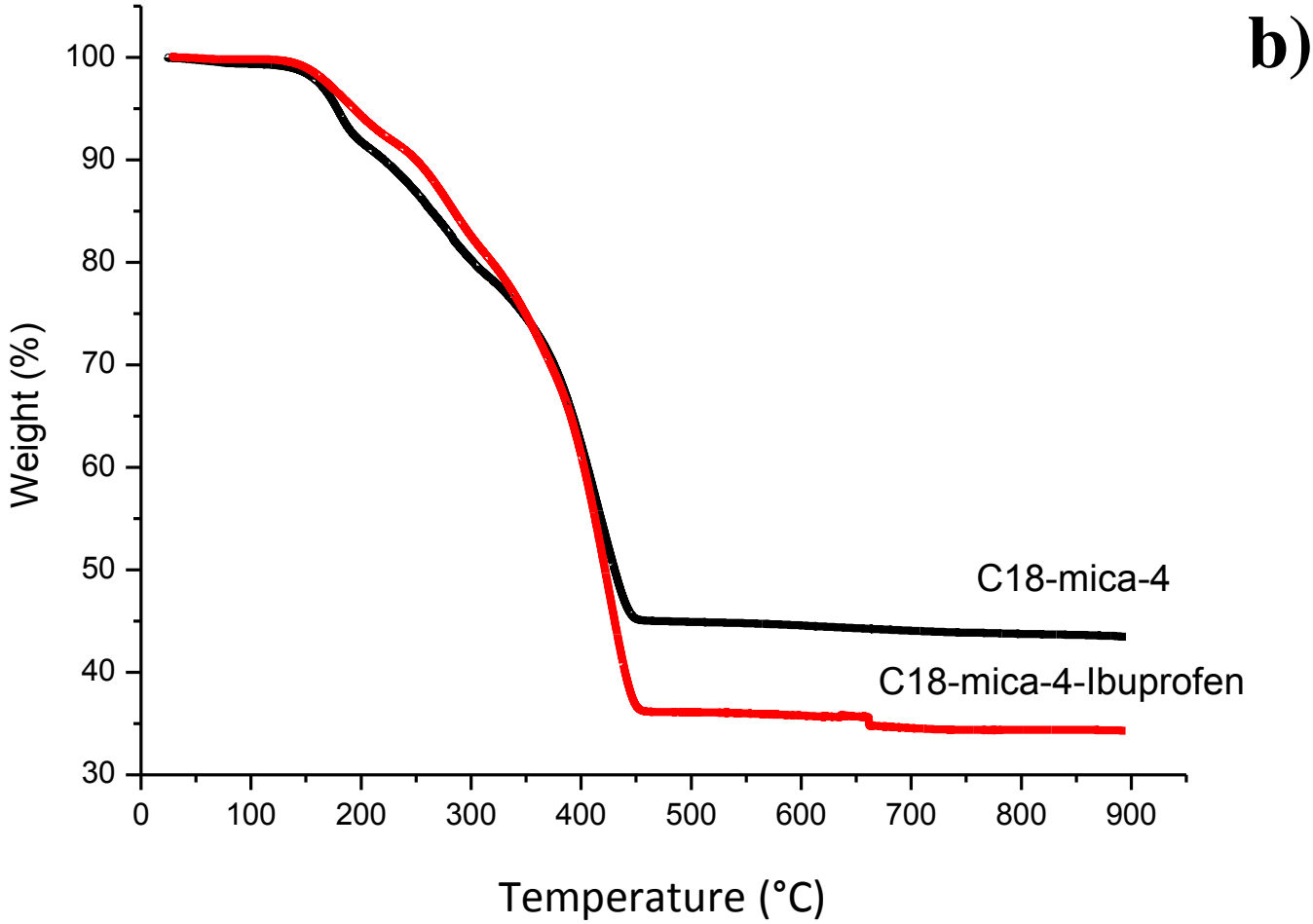

Figure 3

Click here to download Figure: Figure 3_revised.pdf

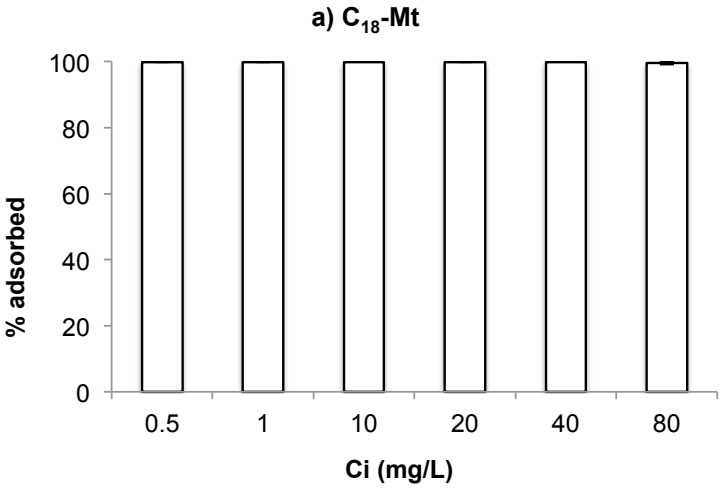

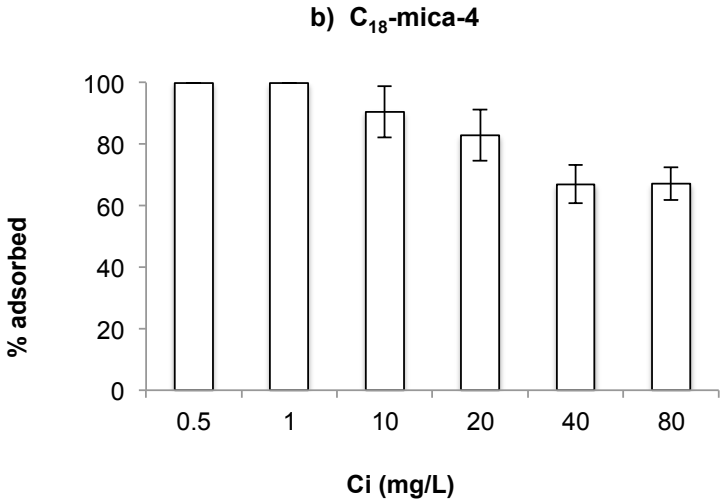

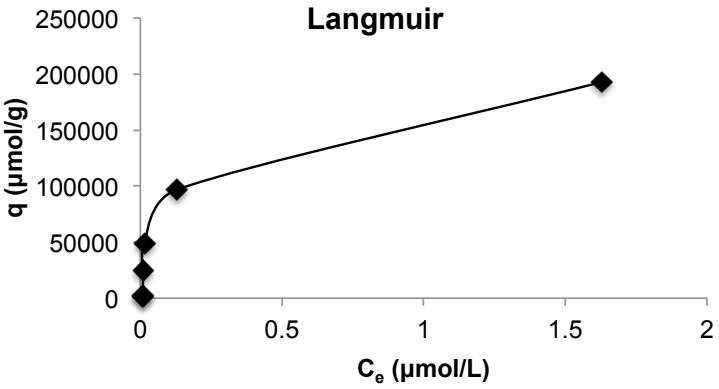

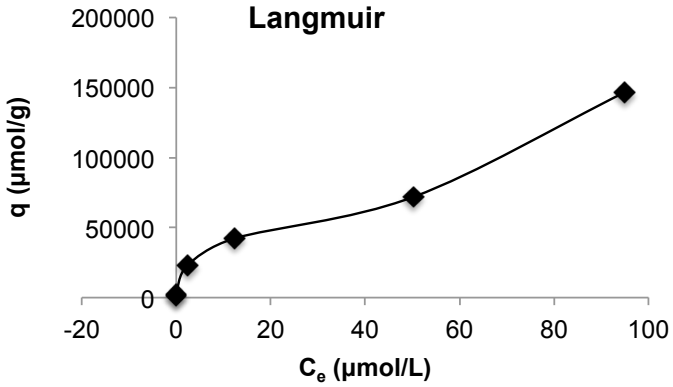

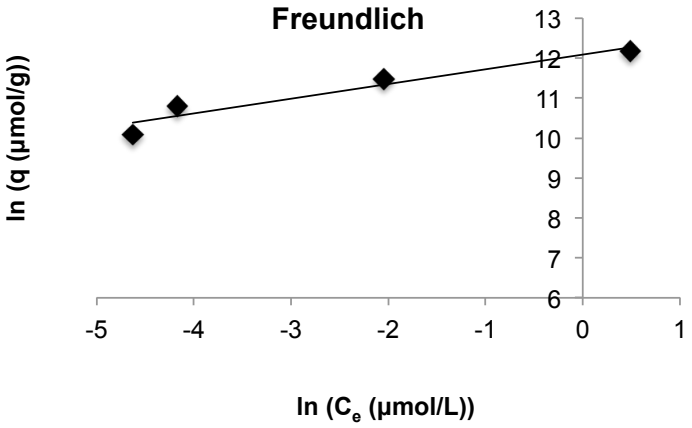

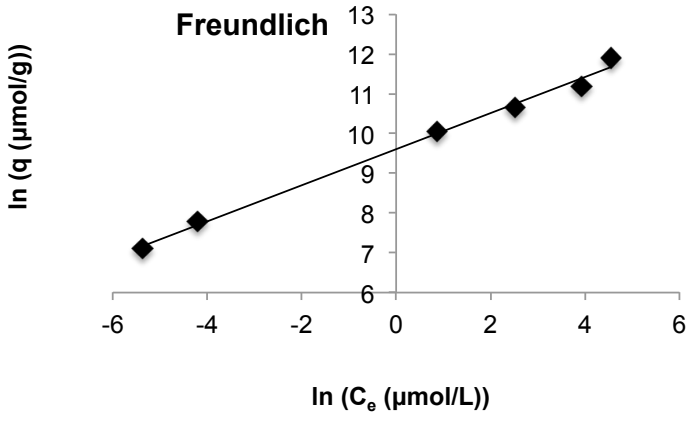

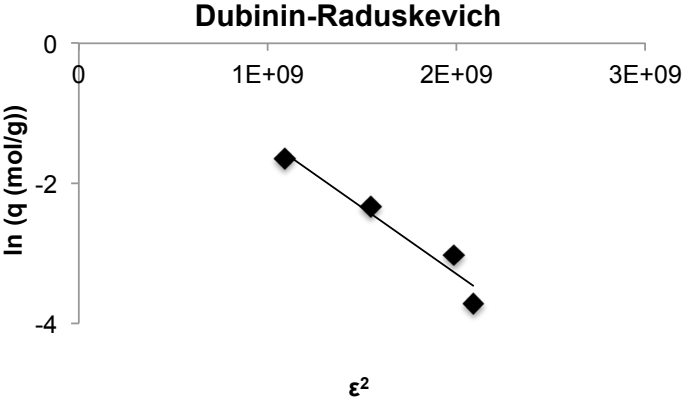

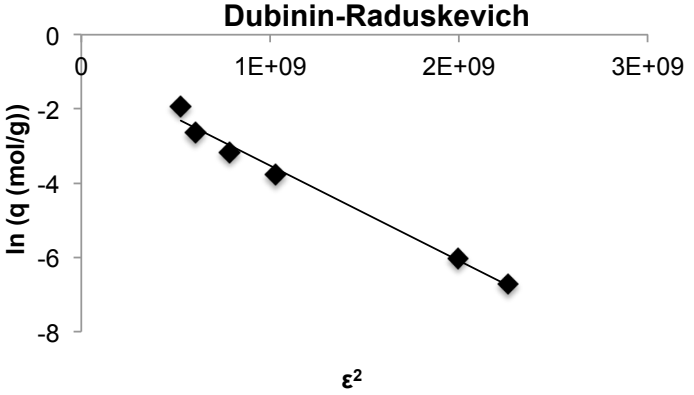

Figure 4

Click here to download Figure: Figure 4_revised.pdf

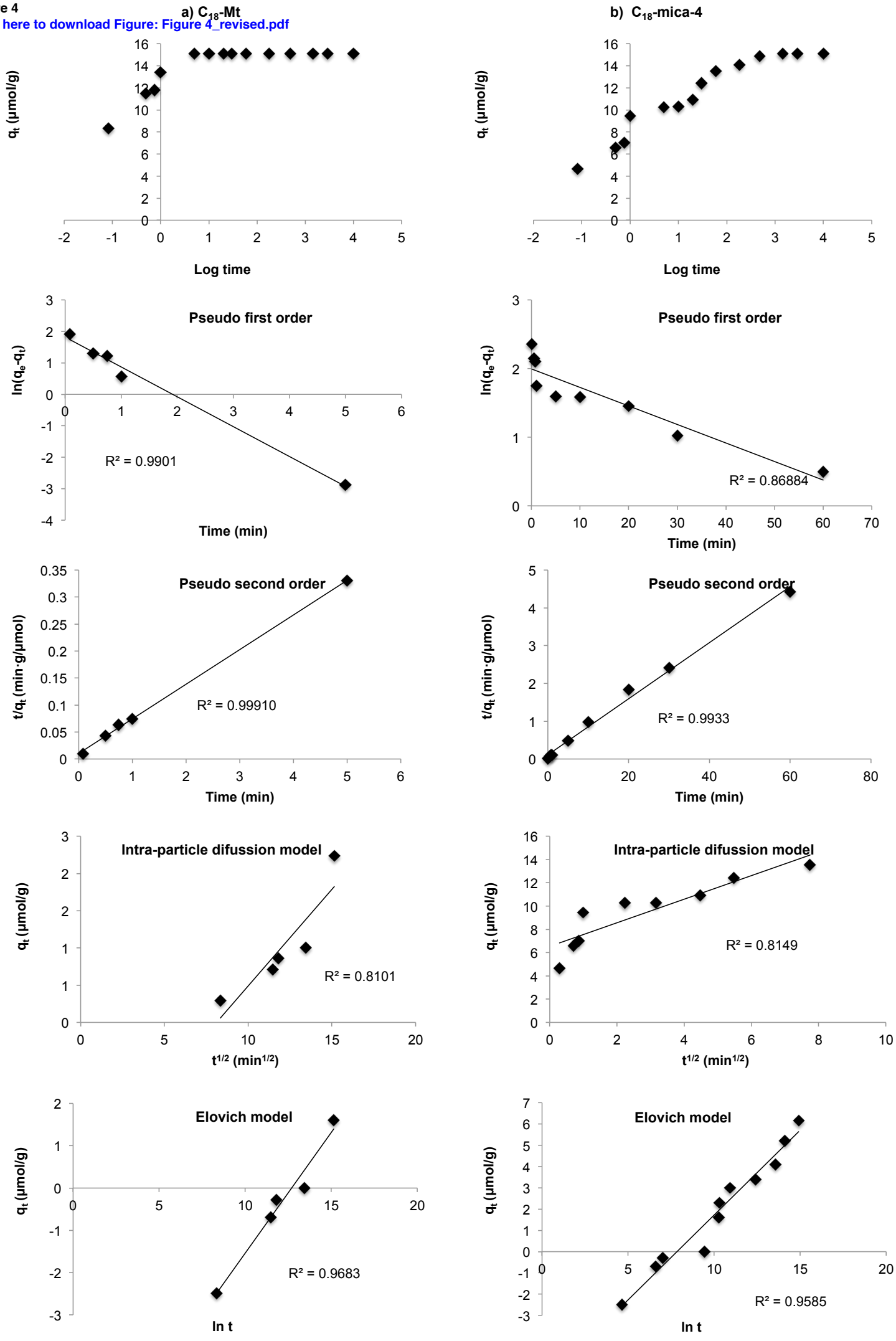

Figure 5

Click here to download Figure: Figure 5_revised.pdf

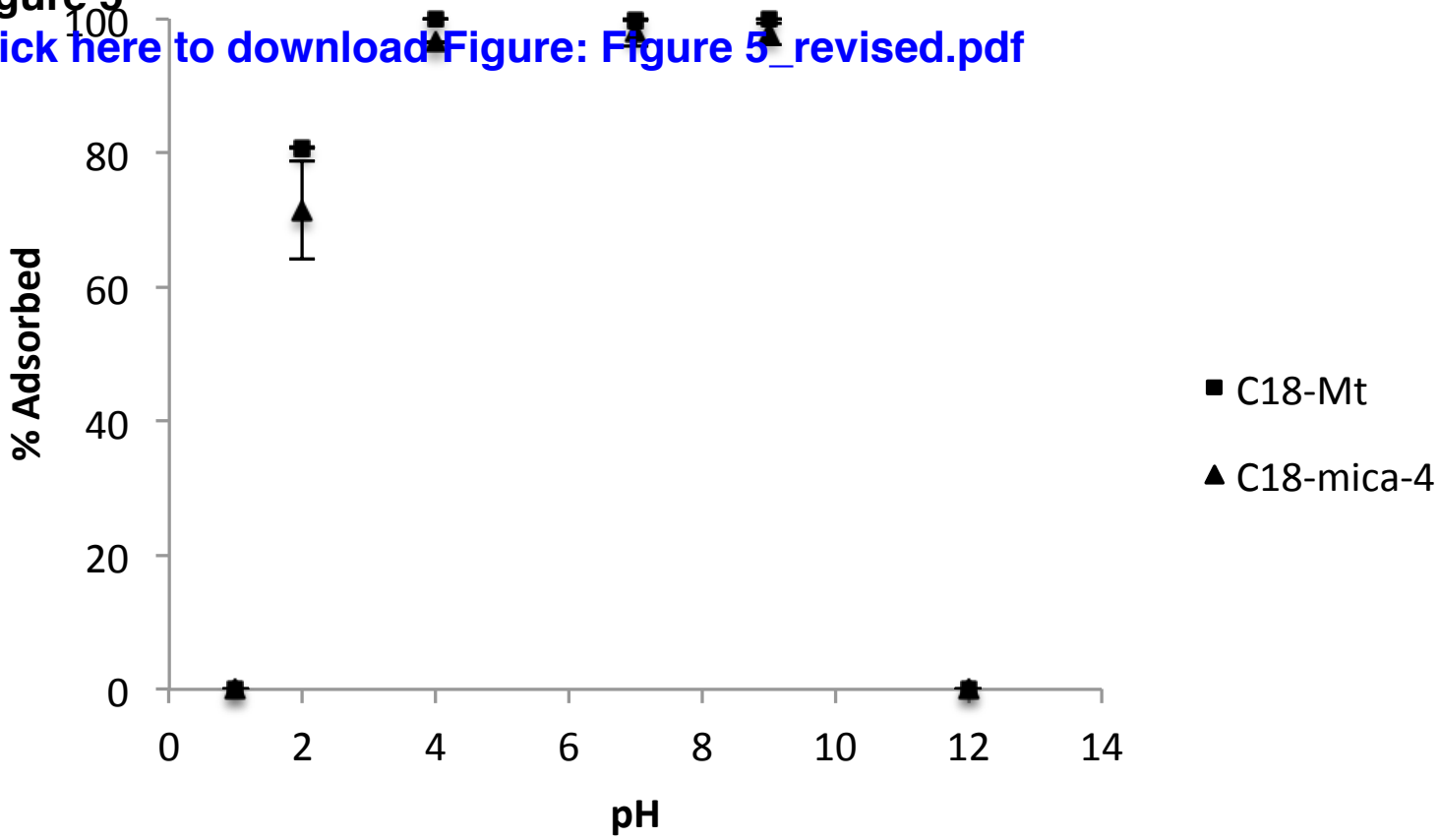

Supplementary Material
Click here to download Figure: Supplementary Material.docx

EVALUATION OF SYNTHETIC AND NATURAL MODIFIED CLAYS FOR THE ADSORPTION OF IBUPROFEN FROM AQUEOUS MEDIA

Julia Martín[1], María del Mar Orta[2*], Santiago Medina-Carrasco[3], Juan Luis Santos[1], Irene Aparicio[1], Esteban Alonso[1]

[1]*Department of Analytical Chemistry, Escuela Politécnica Superior, University of Seville. E–41011 Seville, Spain.*

[2]*Department of Analytical Chemistry, Faculty of Pharmacy, University of Seville, E-41012 Seville, Spain.*

[3]*X-Ray Laboratory (CITIUS), University of Seville, E-41012 Seville, Spain.*

---

*Corresponding author: María del Mar Orta

Address:

Department of Analytical Chemistry, Faculty of Pharmacy, University of Seville, E-41012 Seville, Spain.

E-mail: enmaorta@us.es

Phone-number: +34-9-5455-3804

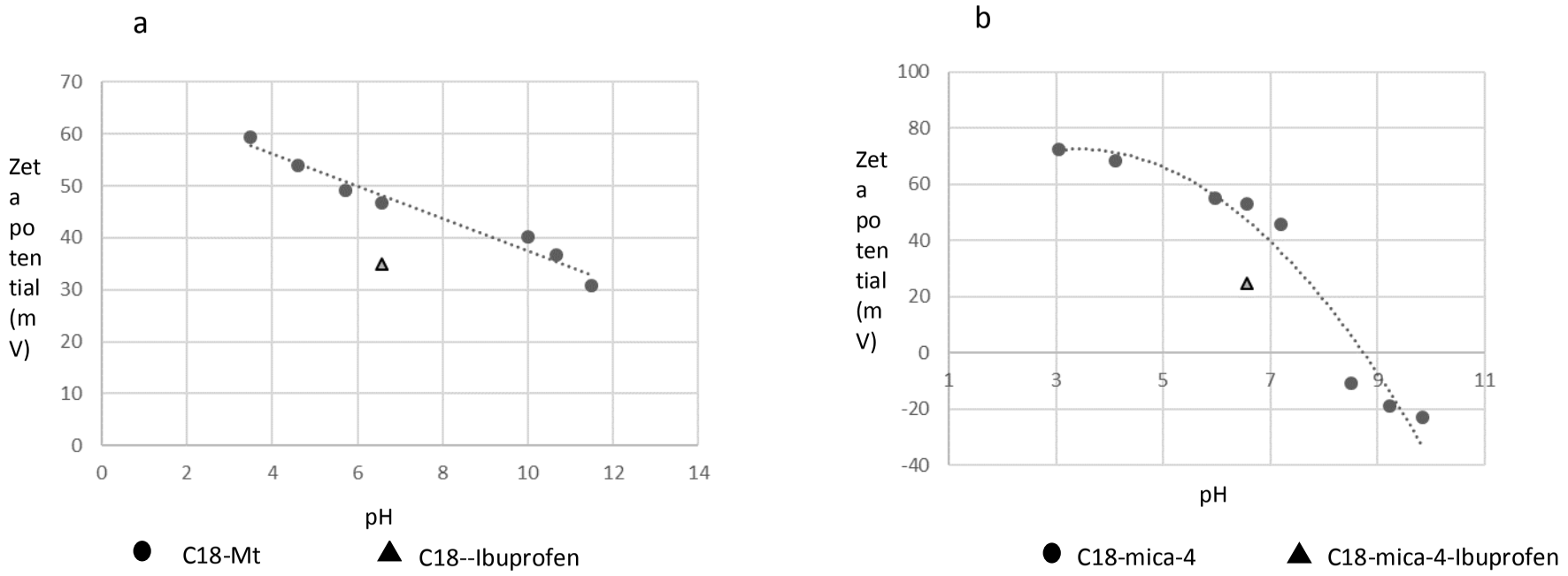

Figure S1. Zeta potential versus pH curves for a) C_{18}-Mt, and b) C_{18}-mica-4 before adsorption experiment; Zeta potential at pH 6.5 for a) C_{18}-Mt-Ibuprofen, and b) C_{18}-mica-Ibuprofen after adsorption experiments.

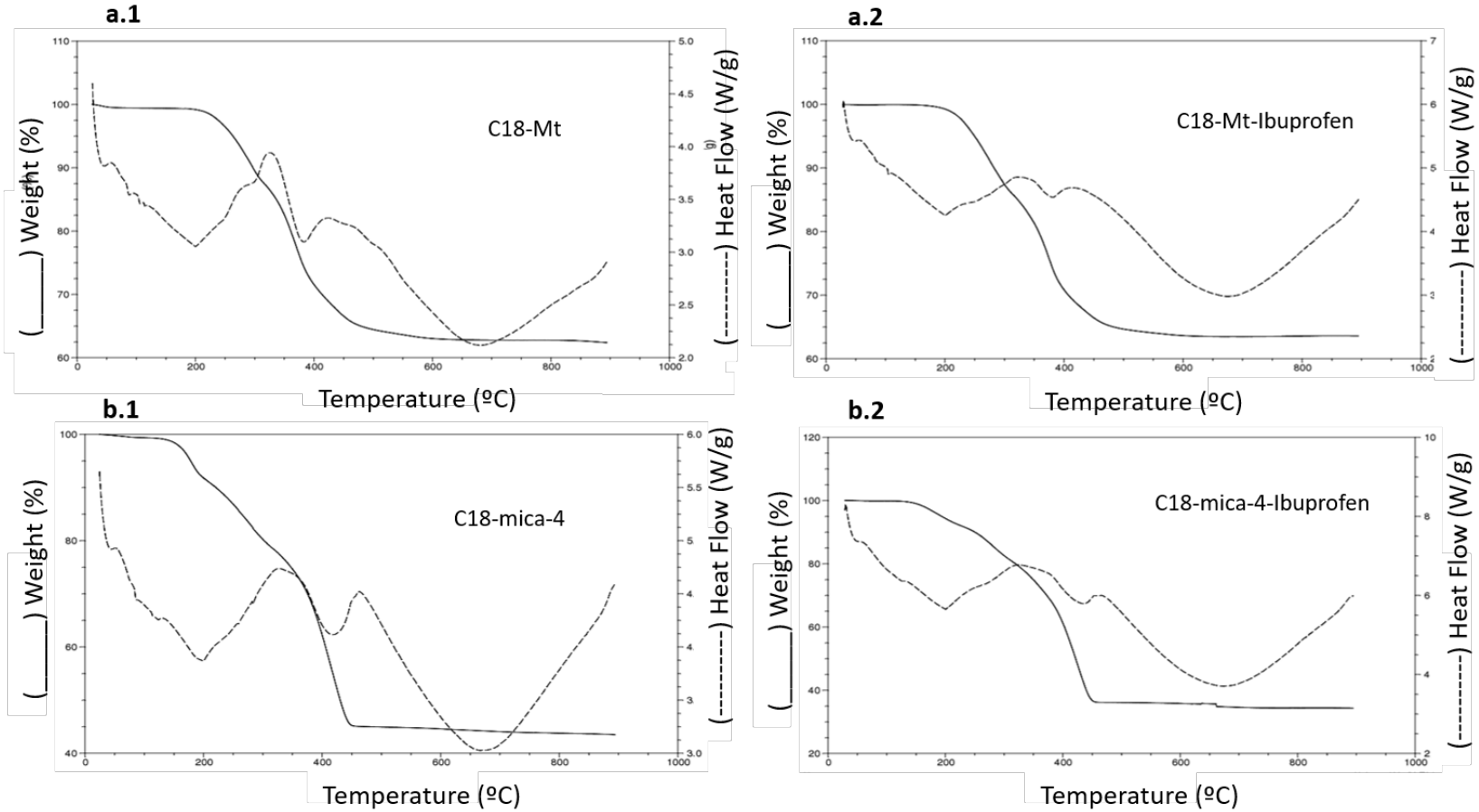

Figure S2. Differential scanning calorimetry and thermal gravimetric analysis for a.1) C_{18}-Mt, a.2) C_{18}-Mt-Ibuprofen, b1) C_{18}-mica-4, and b.2) C_{18}-mica-4-Ibuprofen.